K. Brown (Stanford University)

Properties of Iris-Loaded Guides

Before discussing some of the elementary theory of iris loaded structures a sample list of useful references is given:

Slater, J.C., Rev.Mod.Phys. 20, 473, 1948

Fry and Walkinshaw, Reports in Progress in Phys. XII, 102, 1948-1949

Chodorow et al, R.S.I. 26, 134, 1955

Stanford Linear Accelerator, Hearings for a Congressional Commission of the U.S. Government Printing Office 43633 0, 1959

Ginzton, Hansen and Kennedy, R.S.I. 19, 89, 1948

Chu and Hansen, Journ. Applied Phys. 20, 280, 1949

Journ. Applied Phys. 8, 996, 1947

Loew, G.A., M.L. Report No. 740, Aug. 1960

Neal, R.B., M.L. Report No. 379, March 1957

Leiss, J., Internal memoranda on the Behaviour of Linear Electron Accelerators with beam loading. Internal report - National Bur. of Standards Sept. 1958

Stanford Status Report --- - April 1-June 30, 1959, M.L. Report 640

Neal, R.B., Report 185, Feb. 1953

Chu, E.L., Report 140, Microwave Laboratory, May 1951.

Demos et al, Journ Appl. Phys. 23, 53 (1952)

Stanford Project M Staff Project M Source Book

A rather complete list of references is given by L.Smith in "Handbuch der Physik" band XLIV, 341-389.

Consider the basic structure, illustrated below, of a typical iris loaded waveguide as used for linear electron accelerators.

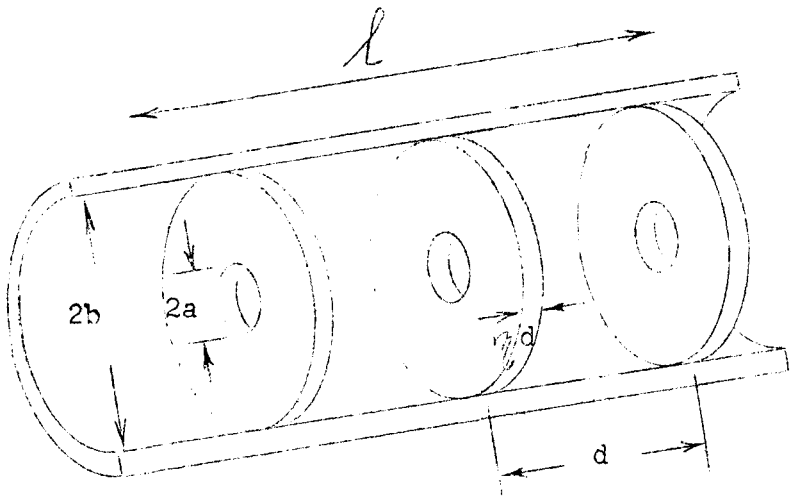

In general this is a circular symmetric waveguide energized in the TM_{01} mode. In traveling wave accelerators usually the $\pi/2$ mode (4 discs per wavelength) are used.

The following parameters (as indicated in the figure above) will have to be chosen: $\lambda, a/\lambda, b/\lambda, d/\lambda$ (refers to either $\frac{\pi}{2}$, $\frac{3\pi}{2}$ or other mode), η d(=t) and the total length ℓ.

The choice of a and b will be affected by the value of the group velocity, v_g (power flow into the structure), i.e., $v_g \simeq F_1(\frac{a}{b})$ and by the value of the desired phase velocity, v_ϕ (velocity of accelerated particle), i.e., $(v_\phi)^{-1} \simeq F_2 (b - a)$.

For optimum values of shunt impedance it is usually desirable that ηd = t shall be as small as is compatible with fabrication. On the other hand for small values of t there is a greater danger of arcing at the disc apertures. An example of the influence of disc thickness on shunt impedance is given in the table below for a few specific cases.* (Values accurate to about ±5 percent)

*It would seem to be very useful to compare these experimental results with calculated values as can be obtained from the work done at Yale University and MURA.

t(inch)	2b(inch)	r/Q	Q	r $\frac{ohms}{cm}$	$v_g/c = \beta_g$
n = 2 (d=2.063 inches, π mode)					
0.061	3.208	60	17000	$5.05\ 10^5$	0
0.120	3.203	61	16900	$5.20\ 10^5$	0
0.230	3.198	61	17200	$5.25\ 10^5$	0
n = 3 (d=1.378 inches, $2\pi/3$ mode)					
0.061	3.216	48	13200	$6.35\ 10^5$	0.0194
0.120	3.214	50	13000	$6.50\ 10^5$	0.0142
0.230	3.213	51	13200	$6.74\ 10^5$	0.0080
n = 4 (d=1.034 inches, $\pi/2$ mode)					
0.061	3.217	54	9100	$5.40\ 10^5$	0.0191
0.120	3.219	53	10100	$5.41\ 10^5$	0.0143
0.230	3.224	51	9950	$4.97\ 10^5$	0.0084

f = 2856 Mc/s; 2a = 0.8225 inches; β_ϕ = 1.0 = normalized phase velocity.

Factors influencing the choice of ℓ are the attainable Q_o of the cavities, the degree of beam loading, frequency, the choice of group velocity and the dimensional tolerances attainable.

Dimensional errors in the structure cause a relative phase shift between the accelerated particles and the traveling wave, consequently a broader energy spectrum at the output and a loss in beam energy. The mathematical details of this will be discussed in the following, here only the conclusions will be given; i.e., that the required dimensional tolerances on 2b for a fractional energy loss smaller than 0.005 is typically of the order of ±0.0002 inches for λ_o = 10.5 cms. These tolerances are attainable with careful machine shop practice. An alternative is, with slightly less rigorous requirements in tolerances to tune each cavity individually by deforming the wall between the irises; however it is not desirable to rely upon this completely - hence, tolerances are usually held as close as possible and the deformation is relied upon only as a final

tuning adjustment.

The fabrication of individual accelerator cavities has developed along different lines. If many identical sections are necessary the process of electroforming (used at Stanford University) is economical and with care produces the desired tolerances. The problems involved are plating the copper in such a way that an oxygen -free copper body is produced to facilitate later soldering and to minimize outgassing of the surfaces. An alternative method, usually employed for commercial linacs, is to solder individual cavities together.

In a proton linear accelerator one would normally encounter a sufficient number of different sections (because of the range in β values) to make the electroforming technique uneconomical compared with the soldering technique.

The selection of the operating mode is guided by several factors of which the value of the shunt impedance is the dominant one. Before treating this in more detail, it is worth while mentioning the following observed phenomena which have bearing on the selection of the operating mode.

In high energy linear accelerators with electron currents in excess of 200 ma. it has been observed that the transmitted beam pulse length may be shortened as a result of radial defocusing effects resulting from a backward wave oscillation in a TM_{11} type mode generated by the beam.

This is illustrated in the following diagram where both characteristics for forward and backward wave are drawn.

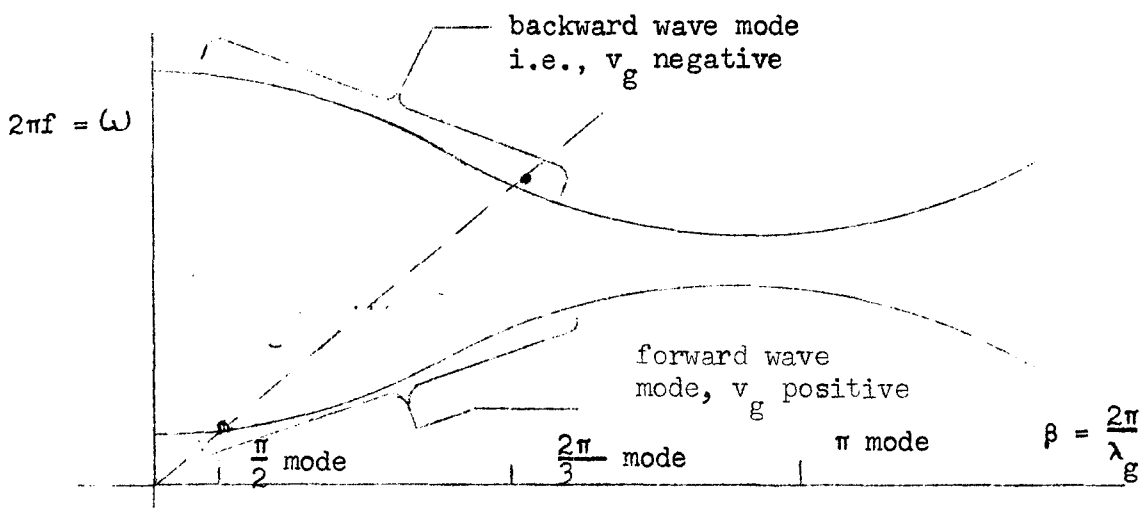

The operating point for the $\frac{\pi}{2}$ mode can coincide with the operating point of a different mode in the backward wave. These difficulties have been minimized by using L band and the $\frac{2\pi}{3}$ mode. This combination has made it possible to go to higher currents and longer pulse lengths before pulse shortening is observed. It is, of course, possible to suppress the TM_{11} mode in the waveguide, but only at the expense of decreasing the Q_o value for the fundamental mode. Also the fabrication tolerance problems arising from mode suppressors are not trivial.

Elementary Theory of Traveling Wave Linacs

The shunt impedance r will be defined here as $r \equiv \frac{E^2}{-dP/dz}$ where E is energy gained per unit length and dP/dz is power dissipated per unit length. An approximate expression for r can now be found and is expressed in the graph below where $r\delta$ is plotted as a function of n, with δ = skin depth; n = number of discs per guide wavelength.

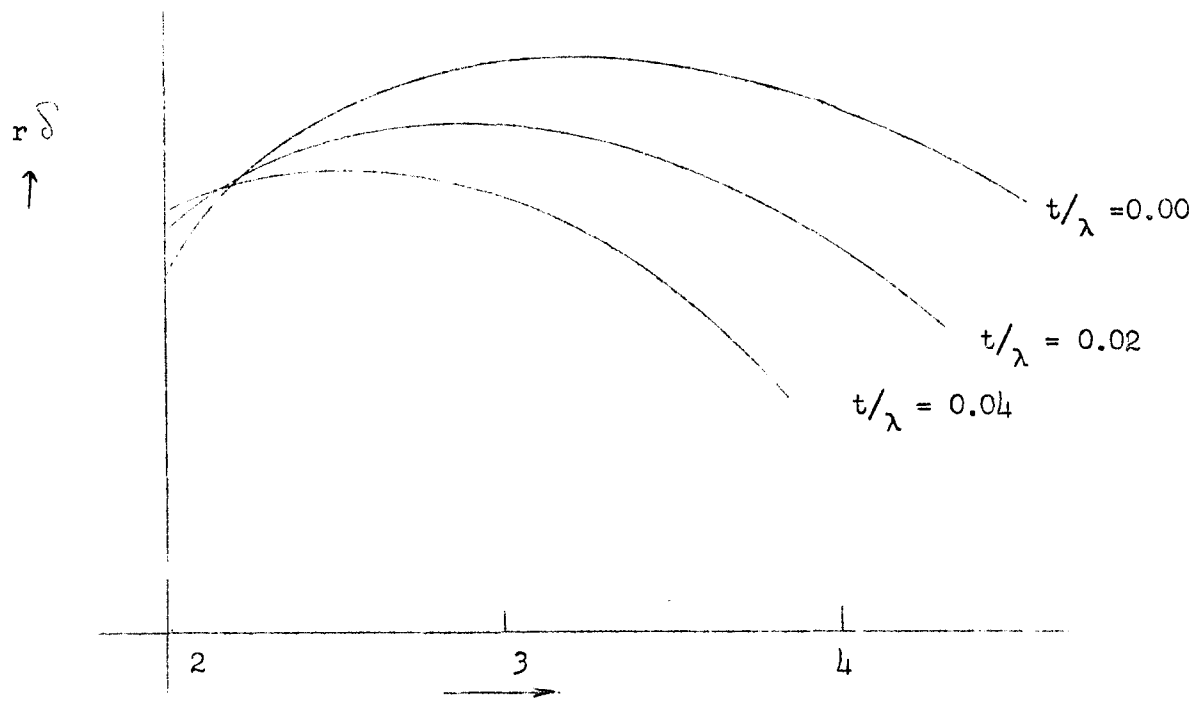

From this graph it is concluded that for $t/\lambda \neq 0$, the optimum number of discs is 3.5 per guide wavelength and for larger thicknesses this shifts to lower values for n.

The Stanford mark IV accelerator uses 3 discs per guide wave length ($\frac{2\pi}{3}$ mode) as will the project M machine.

As a next step the relative merits of traveling wave versus standing wave will be considered.

Taking $P = Wv_g$ where P is the power flow, W is the energy density and v_g is the group velocity and also

$$Q = \frac{\omega W}{\left(-\frac{dW}{dt}\right)} \quad \text{or} \quad Q = \frac{\omega W}{\left(-\frac{dP}{dz}\right)}$$

for a traveling wave structure, it follows then that

$$P(z) = P_o e^{-\left(\omega/v_g Q\right) z}$$

$$\text{or } E(z) = E_o e^{-\left(\omega/2v_g Q\right) z} = E_o e^{-Iz}$$

where $I = \frac{\omega}{2v_g Q}$ defines the electric field attenuation coefficient.

E_o can be rewritten by using the definition of r.

$$r \equiv \frac{E^2}{-\frac{dP}{dz}} = \frac{E^2}{\omega W/Q} = \frac{E^2}{\left(\omega P/v_g Q\right)} = \frac{E^2}{2IP}$$

therefore $E_o = (2 I P_o r)^{1/2}$.

From this the net voltage gain for the traveling wave case can be found, for an accelerator section of length ℓ

$$V_{tr} = \int_o^{\ell} E dz = \sqrt{2(I\ell)\, P_o r \ell}\ \left(\frac{1 - e^{-I\ell}}{I\ell}\right).$$

Optimizing V_{tr} now as a function of $I\ell$ one finds $I\ell = 1.26$ and with this

$$V_{tr} = 0.905 \sqrt{P_o r \ell} \ .$$

This is the optimum voltage gain with light (zero) beam loading. Practical values with light-to-heavy beam loading range as $0.5 < I\ell < 0.9$. The smaller $I\ell$ corresponding to the heavier beam loading.

Comparing this voltage gain with the voltage gain for the standing wave case

$$V_{st} = \sqrt{\frac{P_o \ell r}{2}} \quad *$$

A further point for comparison is the fact that in the standing wave case the field builds up from zero to a steady state value E_s as

$$E = E_s (1 - e^{-\omega t/2Q_L})$$

Therefore, as expected, a built-up time is needed before acceleration; the main point is, however, that for a standing wave accelerator the field never reaches an equilibrium value. For the case of traveling waves a certain delay is also needed before acceleration, given by the filling time t_F which is related to the attenuation constant I as

$$t_F = \frac{2I\ell Q}{\omega}$$

but equilibrium is obtained for $t > t_F$.

Another drawback in the case of a standing wave accelerator is that the impedance presented to the rf power source varies during the build-up time as

$$\frac{Z}{Z_o} = \frac{1 - e^{-\omega t/2Q\ell}}{1 + e^{-\omega t/2Q\ell}}$$

From this: $t = o$ gives $Z = o$, $t = \infty$ gives $Z = Z_o$.
This characteristic can cause difficulties with the rf power sources.

In the above the energy gain (V) has been obtained by assuming zero beam loading. Now this will be taken into account. In the case of synchronous operation (i.e., the particles riding on the crest of the wave) the relevant differential equations are

* In the literature the shunt impedance is sometimes tabulated (for the standing wave case) directly as $(\frac{r}{2})$ instead of r.

$$\frac{dP}{dz} + 2IP + iE = 0$$

and $$\frac{dE}{dz} + IE + Iri = 0$$

with the solutions

$$P(z) = P_o \ell^{-2Iz} + \frac{i^2 r}{2I}(1 - \ell^{-Iz})^2 - 2i\left(\frac{rP_o}{2I}\right)^{1/2}\left(1-\ell^{-Iz}\right)\ell^{-Iz}$$

$$E(z) = E_o \ell^{-Iz} - ir(1 - \ell^{-Iz})$$

These equations hold for synchronous particles. In case the particles are not riding on the wave crest cosΘ terms have to be introduced, in this case, E(z) must be separated into two quadrature components, namely,

$$E_1(z) = E_o \cos\Theta^{-Iz} - ir(i - \ell^{-Iz})$$

and

$$E_2(z) = E_o \sin\Theta \ell^{-Iz} .$$

For the energy gain, only $E_1(z)$ is of concern and from this $V = \int_o^{\ell} E_1 \, dz$ gives

$$V = E_o \ell \cos\Theta\left(\frac{1-\ell^{-I\ell}}{I\ell}\right) - ir\ell\left(1 - \frac{1-\ell^{-I\ell}}{I\ell}\right)$$

It is useful here to define an expression $R \equiv \left(\frac{E_o^2}{P}\right)\ell^2$

or $R \equiv \frac{r}{Q}\frac{\omega}{v_g}\ell^2$ (using the definitions for Q, P and r).

This substituted yields

$$V = (P_o R)^{1/2}\cos\Theta\left(\frac{1-\ell^{-I\ell}}{I\ell}\right) - \frac{iR}{4}\left[1 - \frac{I\ell}{3} + \frac{(I\ell)^2}{12} - \frac{(I\ell)^3}{60} + \ldots\right]$$

Remembering that $I \equiv \frac{\omega}{2v_g Q}$ one finds for high Q values, and consequently small $I\ell$ values

$$V \cong \left(\sqrt{P_o R}\right)\left(\cos\Theta\right) - iR/4$$

Assuming $\cos\theta = 1$, V can be optimized as a function of R resulting in

$\left(\text{with } R = \frac{4P_o}{i^2}\right)$,

$$V = P_o/i$$

similarly $E = E_o\,(1 - z/\ell\,)$ $\qquad (Q \to \infty \text{ or } I \to 0)$

and $\ell = 2P_o/iE_o$.

This determines optimum section length depending on what field gradients are tolerable and what rf power sources are available.

From the above, group velocity and filling time can be simply evaluated and are given by

$$v_g = C\left(\frac{P_o}{E_o^{\,2}}\right)\left(\frac{r}{Q}\right)\left(\frac{2\pi}{\lambda}\right)$$

$$t_F = \ell/v_g = \left(\frac{E_o}{i}\right)\left(\frac{\lambda}{\pi c}\right)\left(\frac{r}{Q}\right)^{-1}$$

Using the equations derived thus far and assuming a 1 megawatt power source (P_o) and current loading of 1 ma. (i)

for $Q \to \infty$ or $I\ell \to 0$

then V = 1 Bev

$\ell \cong 333$ ft.

$t_F \cong 424$ μsec

$\beta_g \cong (1300)^{-1}$ This value of β_g is too low because of the tolerances demanded in this case.

Therefore, these figures are obviously impractical.

Assume $E_{ave} = 10^5$ volts/cm = 3 Mev/ft. which is practical,

and $\beta_g = (100)^{-1}$ allowing reasonable tolerances,

then $P_o = 12.7$ megawatts

$t_F = \frac{0.424}{i}$ μsec and with the choice of i = 0.424A

$t_F = 1$ μsec

V = 30 Mev

$\ell = 10$ ft.

Other examples may be easily evaluated from the preceeding equations. However, it is easy to conclude that if extremely high Q's can be obtained, the standing wave machine becomes of considerable interest again as compared to the traveling wave case. This is particularly true of machines having peak beam currents $\lesssim$ 1 ampere. In the event that high Q's become attainable, a CW standing wave machine would be of considerable interest since high average power microwave sources are already available. Clearly there are many practical problems that must be solved in such an event, but the possibility should not be overlooked.

Going back to the case where Q is finite, as has been stated previously, the optimization for $I\ell$ depends upon the degree of beam loading. Included below are two tables taken from the Project M source book which illustrates the choice of design parameters for a 10 percent* beam loaded electron linac. The first table shows the effect of frequency upon the choice of machine parameters. The second table gives typical values of design parameters for a 10 Bev linac ($\beta_\phi = 1$) for 3 different frequencies. In the case of a proton linac the current would be less than quoted here but the remaining figures should be substantially the same.

* Ten percent beam loading here means the full load energy is 0.9 of the no load energy.

Table 1

Frequency dependence of principal machine parameters.

Parameter	Frequency Dependence	Frequency Preference High	Frequency Preference Low	Notes
shunt impedance per unit unit length (r)	$f^{1/2}$	X		(1)
rf loss factor (Q)	$f^{-1/2}$		X	(1)
filling time (t_f)	$f^{-3/2}$	X		(1), (2)
total rf peak power	$f^{-1/2}$	X		(1), (2), (3)
rf feed interval (ℓ)	$f^{-3/2}$		X	(1), (2)
number of rf feeds	$f^{3/2}$		X	(1), (2), (4)
rf peak power per feed	f^{-2}	X		(1), (2), (3)
rf energy stored in accelerator	f^{-2}	X		(1), (2), (3)
beam loading (-dV/di)	$f^{1/2}$		X	(1), (2), (4)
maximum peak beam current	$f^{-1/2}$		X	(1), (2), (3), (6)
diameter of beam aperature	f^{-1}		X	(1)
max. rf power available from single source	f^{-2}		X	(5)
max. permissible electric field strength	$f^{1/2}$	X		(7)
relative frequency and dimensional tolerances	$f^{1/2}$	X		(1), (2)
absolute frequency and dimensional tolerances	$f^{-1/2}$		X	(1), (2)
power dissipation capability of accelerator structure	f^{-1}		X	(1), (2), (4)

Notes:
1. For direct scaling of modular dimensions of accelerator structure.
2. For same rf attenuation in accelerator section between feeds.
3. For fixed electron energy and total length.
4. For fixed total length.
5. When limited by cathode emission.
6. When limited by beam loading.
7. Approximate; empirical.

Table 2

Design parameters of a 10 Bev electron accelerator at 3 frequencies.[1]

	Frequency		
	(L-Band) 1000 Mc/sec	(S-Band) 3000 Mc/sec	(X-Band) 9000 Mc/sec
shunt impedance per unit length (r)	0.27×10^6	0.47×10^6	0.81×10^6 ohms/cm
rf loss factor (Q)	2.25×10^4	1.3×10^4	0.75×10^4
filling time (t_F)	4.52	0.87	0.17 μsec
total rf peak power	2490	1440	830 Mw
rf feed interval	52	10	1.92 ft.
number of rf feeds	185	960	5000
rf peak power per feed	13.5	1.5	0.17 Mw
rf energy stored in accelerator	6580	731	81 joules
rf energy required for 1.63 μsec electron beam pulse length	15,300	3600	1500 joules
total average rf power at 360 pulses/sec	5.50	1.30	0.54 Mw
beam loading (-dV/di) for max beam power	19.6	34.2	59 Bev/amp
50 percent beam loading: max peak beam current	294	170	98 ma
diameter of beam aperture	2.670	0.890	0.297 inch
max rf peak power available from single source	216	24	2.7 Mw
max permissible electric field strength[2]	133	230	398 kv/cm
max expanded beam energy[3]	29.3	50.7	87.6 Bev
relative frequency and dimensional tolerances[4]	0.98×10^{-5}	1.70×10^{-5}	2.94×10^{-5}
absolute frequency and dimensional tolerances[4]	87 kc/sec; 0.09 mils	50 kc/sec; 0.05 mils	29 kc/sec; 0.03 mils
average power dissipated per unit area of accelerator surface[5]	0.17	0.12	0.15 watts/cm^2
average temperature difference across accelerator wall[6]	0.55	0.13	0.05 degrees C

1. Assumptions: $2\pi/3$ mode: $I\ell = 0.6$ nepers (rf attenuation); $V_0 = 11.6$ Bev (no-load beam energy); L = 9600 feet; direct scaling of modular dimensions.
2. Based on max gradient obtained to date at S-band, values for other frequencies based on scaling as $f^{1/2}$.
3. As limited by maximum permissible field strength.
4. For one per cent loss in beam energy.
5. Based on 360 pulses per second and 1.63 μsec electron beam pulse length.
6. Based on copper wall 1/3, 1, and 3 cm thick at X-, S-, and L-bands, respectively.

If higher average energy gradients are desired, it is desirable to use accelerator sections which are geometrically not identical. In this case, a design of non-uniform geometry but constant axial fields (i.e., constant gradient) over the full length of the structure becomes interesting. Normally with repetitive geometries there is an exponential decay of axial field with distance from the rf power source.

The ratio of peak-to-average field in the repetitive structure may be as high as 1.76 although in practice the ratio is more likely to be of the order of 1.4 because of the choice of $I\ell$. Therefore higher energies by this factor could be obtained with the constant gradient structure before similar voltage breakdown problems are encountered.

At present the uniform structure accelerator is chosen at Stanford for the Mark IV accelerator, however, a point-by-point comparison suggests that a constant gradient structure merits further consideration.

Some discussion regarding shunt impedance versus the normalized phase velocity β_ϕ of disc loaded structures.

The table below shows some experimental values of shunt impedance obtained for a disk loaded structure at S-band frequencies and for the $2\pi/3$ mode (per guide wavelength).

β_ϕ	Q_o	r/Q_o	r
1.0	13000	47 ohms/cm	$6.1\ 10^5$ ohms/cm
0.45	12500	45	$5.65\ 10^5$
0.40	12050	42.5	$5.12\ 10^5$
0.85	11500	40.0	$4.60\ 10^5$
0.80	11000	36.9	$4.06\ 10^5$
0.75	10400	33.5	$3.48\ 10^5$
0.70	9800	29.7	$2.91\ 10^5$
0.65	9130	25.7	$2.35\ 10^5$
0.60	8470	21.0	$1.78\ 10^5$
0.55	7700	16.7	$1.29\ 10^5$
0.50	6930	12.2	$8.47\ 10^4$

$\beta_\phi = \frac{v_\phi}{c}$ = normalized phase velocity

This table was evaluated by measuring all $r/_Q$ values to an accuracy of ±5 percent for the respective β_ϕ

The Q values were calculated and then normalized to the measured value of Q at $\beta_\phi = 1$. This means that for example at $\beta = 1/2$ the r values have an accuracy of approximately 10 percent at best.(Q values ± 5 percent)

That the Q values decrease for lower phase velocities can be explained qualitatively by the fact that (b - a) becomes greater and consequently there is a larger surface area and current concentration near the aperture edge, resulting in a lower Q value.

Tolerances

Variations in frequency, temperature, axial field strength, input rf phase and dimensional errors all have an influence on the performance of the Linac. In general most of these errors may be expressed as an equivalent phase slip between particle and traveling wave with a consequent beam energy spread at the output and a beam energy loss.

The fractional beam energy loss due to a frequency change $df/_f$ is given by

$$\frac{\delta V_o}{V_o} = -\frac{1}{6}(\delta\phi)^2\left\{\frac{6}{(I\ell)^2} - \frac{3I\ell+6}{I\ell(e^{I\ell}-1)}\right\}$$

where

$$\delta\phi = 2I\ell\, Q\,\frac{df}{f}$$

Substituting some typical values in this equation one finds that in order to keep $\left(\frac{\delta V_o}{V_o}\right) \leq 0.005$ it is necessary to keep $\delta f < 35$ kc/s.

The total phase shift deviation due to dimensional errors in individual cavities should be assessed on the basis of an accumulation of random errors, neglecting here systematic errors. Considering now the phase shift error per cavity for a $\frac{2\pi}{3}$ mode

$$\delta\phi_{p.c.} = 120\,\frac{c}{v_g}\left\{\frac{\delta(2b)}{2b}\right\}$$

One finds if $\delta\phi_{p.c.}$ maximum is taken as 0.6^0, in connection with the maximum tolerable energy spread, that the required dimensional tolerances are ±0.0002 inches. In this case the total accumulated phase shift, due to random errors is $\delta\phi_{tot} = \sqrt{N}\,\delta\phi_{p.c.}$ where N is the number of cavities. Also temperature variations in the accelerator structure have to be closely controlled. A rise in temperature causes an increase in the resistivity of the accelerator wall with a consequent decrease of Q and r, but of greater importance, the cavity dimensions increase, with a consequent drop in phase velocity (assuming f = constant), resulting in a phase slip between particles and the traveling wave.

The following simple expression gives the influence of temperature on operating frequency:

$$\frac{\delta f}{f} = -\,g\,\delta T$$ where g is the linear coefficient of expansion of the material of the cavity wall. Referring back to the expression for fractional beam energy loss due to $\frac{\delta f}{f}$ one finds for $\left|\frac{\delta V}{V_o}\right| \leq 0.005$ that temperature variations should not exceed 0.8^oC. (using the g value for copper).

The phasing of the individual cavities can be accomplished as follows. The phase slippage of the individual sections can be vectorily analyzed (see diagram) and transferred to an energy error, i.e.

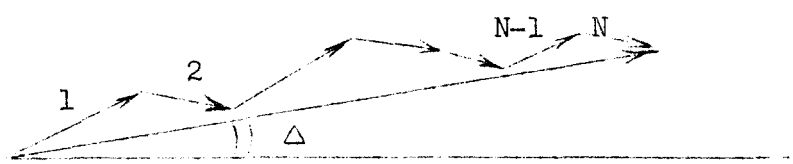

Then $\frac{\Delta E}{E} = \frac{1}{2}\left(\frac{\theta}{2} + (\Delta)\right)^2$ = the spectrum width.

At the output of the accelerator (in the Stanford case) a beam analyzer is used and the collector current can be expressed as

$$\frac{I}{I_o} = \left[\frac{1}{(1+2\,\Delta/\theta)^2}\right]\left[\frac{(1+4\,\Delta/\theta)}{(1+2\,\Delta/\theta)^2}\right]$$

where $I = I_o$ for $\Delta = 0$ and θ = phase spread of the bunched electrons. As can be seen from the vector diagram above it is only necessary in general to phase section N to make $\Delta = o$. The whole accelerator may be optimized in successive steps by changing the phase in each section to optimize the output and each time making $\Delta = o$ by changing the phase in section N. The procedure will converge to the correct solution and should result in a correctly phased machine.

As a concluding remark it should be stated that the arguments brought forward above might not necessarily apply directly to a proton linear accelerator. The basic difference lies in the $\gamma = (1 - \beta^2)^{-1/2}$ of the particles in question.